Hydrogen production from Hydrogen Sulfide Wastestream using Ru/Cd$_{0.6}$Zn$_{0.4}$S Photocatalyst

Thangam N, Suganya Devi B, Lalitha Muthu AC

Abstract— The depletion of non-renewable energy source and increasing levels of environmental pollution are both becoming serious global concerns. The conversion of solar energy into hydrogen via H_2S splitting process assisted by semiconductor photocatalysts is one of the most attractive and focused way of achieving clean and renewable energy systems. A novel Ru $^{2+}$ doped Cd$_{0.6}$Z$_{0.4}$S nanophotocatalyst was synthesized by co-precipitation method. The physical characterization of the nanophotocatalyst had been carried out by XRD, SEM, UV-DRS and EDS. The XRD patterns showed that a new structural peak was found instead of original peaks with mixture of Ru doped Cd$_{0.6}$Z$_{0.4}$S having a particle size of 4.9 nm. The band gap energy of 2.61 eV and threshold wavelength of 475 nm were found using UV-DRS.The photocatalytic generation of H_2 from simulated sulfide wastewater under visible light irradiation were conducted with two different reactors viz., trapezoidal and cylindrical tapered bottom reactors. The comparison of performance also reveals that the trapezoidal reactor produce higher rate of H_2 production (4063 µmol/h) than the cylindrical tapered bottom reactor (3169 µmol/h). The quantum efficiency of 10.1% at 560 nm was found in trapezoidal reactor. This composite exhibited much higher photocatalytic activity for the generation of hydrogen (H_2).

Index Terms— Co-precipitation, Hydrogen, Nano photo catalyst visible light.

I. INTRODUCTION

Hydrogen sulfide (H_2S) is a toxic gas harmful to human beings and the environment. H_2S and sulfide wastewater cause an odour nuisance at low concentration. It is a toxic substance with a characteristic rotten egg smell that can undergo a number of oxidation reactions [Priya and Kanmani, 2008]. H_2S gas and sulfide wastewater is generated from petroleum refineries, sewage treatment Plant, tanning of hides and pulp and paper industries. H_2S is available in millions of tons of quantities in petroleum refineries [Gurunathan et al., 2008 and Preethi and Kanmani, 2012]. If the pH is less than 6, then H_2S is mainly in the gaseous form. When pH increases to $6 - 8$, part of H_2S converts into hydrosulfide ion (HS$^-$). At pH $6 - 8$, there is a mixture of H_2S and HS$^-$. For a pH of $8 - 12$, the main ion is HS$^-$ but there is still some H_2S. The sulfide ions are present in appreciable concentrations above pH 10 [Priya and Kanmani, 2008 and Linkous et al., 2006]. Present removal methods of sulfide removal from industrial wastewater are biological and chemical methods have some drawbacks. The

N.Thangam, Department of Civil Engineering, SRR Engineering College , Chennai , India,).
B. suganya Devi, Department of Civil Engineering, SRR Engineering College, Chennai, India,
A.C.Lalitha Muthu, Department of Civil Engineering, SRR Engineering College, Chennai, India,

new emerging techniques viz., thermochemical, electrochemical and photochemical method also have some drawbacks. During the past three decades, an intense research on economically viable routes of solar energy conversion using semiconductor photocatalyst [Gurunathan et al., 2008]. H_2 has attracted much attention as one of the key components for solving environmental and energy problems all over the world. The conversion of solar energy into hydrogen via H_2S splitting process assisted by semiconductor photocatalysts is one of the most attractive and focused ways of achieving clean and renewable energy systems [Niranjan Biswal et al., 2011]. In recent year, renewable hydrogen production as potentially efficient, environmentally friendly and low cost methods [Nada et al., 2008]. From the fundamental point of view, the cleavage of H_2S is easier than H_2O requiring Gibbs free energy of only 39.4 KJ/mol, which is much less than 284.7 KJ/mol required for water splitting [Priya and Kanmani, 2010]. Nevertheless, the current performance of this process is not sufficient for its implementation at an industrial scale. Accordingly, there is need of developing new catalysts to improve the production of hydrogen under solar radiation. Taking the solar spectrum into account, it is indispensable to develop visible light driven photocatalysts instead of the photocatalysts responding only to ultraviolet light. Unfortunately, there are just a few of photocatalysts that can work efficiently under visible light irradiation [Xianghui Zhang et al., 2010].

Among all the visible-light-sensitive photocatalytic materials developed so far, CdS is one of the most active photocatalyst owing to its suitable band gap (2.4 eV) and their band gap lies in visible region of the solar spectrum [Xiaojing Liu et al., 2011]. It has reported that a combination of two semiconductors (lies in the visible region and lies in the UV region) can be used very effectively for H_2S decomposition. ZnS (2.7 eV) has band gap energy lies in the UV region light [Supriya et al., 1997]. It has reported that a combination of two semiconductors (lies in the visible region and lies in the UV region) can be used very effectively for H_2S decomposition. ZnS (2.7 eV) has band gap energy lies in the UV region light [Supriya et al., 1997].]. No hydrogen was detected when ZnS alone was used as the catalyst even after 5 h of the visible light irradiation, suggesting that ZnS is not active under visible light for photocatalytic H_2 evolution. On the other hand, the activity of CdS was low, in which the photocatalytic H_2 evolution rate [Lu Wang et al., 2010]. The Cd$_{1-x}$Z$_x$S solid solution can solve these problems to some extent, nevertheless there is still a shortcoming, that is, when the value of x is low, the band gap of the solid solution is wide, and when the value is high, the level of conduction band is low which leads to weak photocatalytic without Ru cocatalyst [Guanji Liu et al., 2008]. It has been reported that the photocatalytic properties of CdS could be modified by mixing with the band gap semiconductors, for example ZnS

to form $Cd_{1-x}Z_xS$ solid solution by adjusting the value of (x=0.4) with controlled band gap and light absorption [Naixu Li et al., 2013]. The $Cd_{0.6}Z_{0.4}S$ solid solutions have been evident as efficient photocatalysts with doping a noble metal in the presence of sacrificial electron donor. It was found that doping of foreign element Ru^{2+} enhances the photocatalytic activity by forming the dopant impurity levels for better charge separation [Yabo Wang et al., 2012].

In the current study, it is reported that Ru doped $Cd_{0.6}Z_{0.4}S$ nanophotocatalyst was prepared by co-precipitation method. The prepared photocatalyst was characterized by XRD (particle size), SEM (morphology), EDS (elemental composition) and UV-DRS (band gap energy). In order to study the effects of operating parameters viz., sulfide/sulfite ion concentration, pH, catalyst dosage, volume of simulated sulfide wastewater and light intensity for the photocatalytic generation of H_2 under visible light irradiation.

II. EXPERIMENTAL

A. Preparation of photocatalysis

All of the chemical reagents were analytical grade and used without further purification.

Synthesis of Cd$_{0.6}$Z$_{0.4}$S nanocomposite

The $Cd_{0.6}Z_{0.4}S$ were prepared using co-precipitation method by adding Na_2S into a 500 mL of distilled H_2O containing $(Cd(CH_3COO)_2)$ and $(Zn(CH_3COO)_2)$. The whole process was carried out under magnetic stirring. After 1 h, yellow precipitate was formed for cadmium and zinc sulfide solutions. After 24 h, the solution was removed from stirring condition and washed with isopropyl alcohol and distilled H_2O to split particles from each other. The precipitate was allowed to settle and dried in oven for 110ºC.

Synthesis of Cd$_{0.6}$Zn$_{0.4}$S/Ru photocatalyst

Initially $RuCl_2$ (1% wt) powder and 5-6 drops of hydrochloric acid was added to $Cd_{0.6}Z_{0.4}S$ nanophotocatalyst. Then the prepared catalyst was kept in ultra sonication for 10 minutes, the resulting paste was dried at 150°C for 2 h and was subsequently calcined at 350°C for 1.5 h to form $Ru/Cd_{0.6}Z_{0.4}S$ nanophotocatalyst.

B. Characterization of photocatalyst

The prepared photocatalyst was characterized by the X-ray diffraction (XRD) patterns were recorded using diffractometer in the range of 10 – 80 degrees. The ultra violet visible diffuse reflectance spectrum (UV-visible DRS) was recorded using spectrophotometer in the spectral range of 200-800 nm. The scanning electron micrographs (SEM) were measured using microscope and Energy dispersive X-ray spectroscopy (EDX) was measured using spectroscopy to found the elemental composition present in that photocatalyst.

C. Photocatalytic H$_2$ production

The experiment was conducted in photocatalytic reactor of 500 mL capacity was irradiated using halogen lamp. The reactor has two inlets. One inlet was used for purging of nitrogen (N_2) gas and the other hole to collect H_2 gas by downward displacement jar as shown in (Fig. 1). Nitrogen

was purged through the inlet before the reaction to remove oxygen. The light source was 300 W halogen lamps. The photocatalyst powders of 0.2 g were dispersed by peristaltic pump in an aqueous solution 100 mL containing 0.2 M Na_2S and 0.25 M Na_2SO_3. The temperature of the photoreactor was maintained at room temperature. The H_2 generation was collected in a water displacement jar and determined by GC (Shimadzu 14B, Molecular sieve -5 A column, TCD detector and N_2 carrier gas).

The apparent quantum yield (Q.Y.) at 560 nm was determined for the photocatalytic system with an interference filter. Q.Y. in % was calculated using the following equation:

Q.Y. (%) = (Number of evolved H_2 molecules / Number of incident photons) x 100
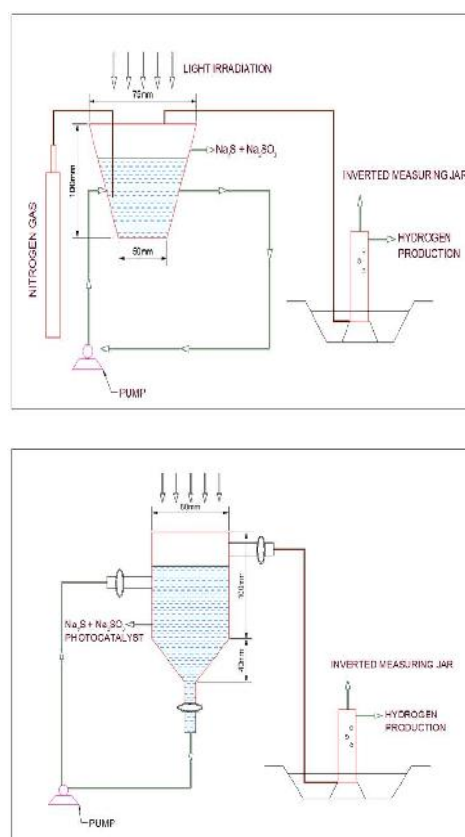

Fig.1. The reactor layout used for photocatalytic H_2 production

III. RESULT AND DISCUSSION

A. XRD CHARACTERIZATION(PARTICLES SIZE)

In Fig. 2 and 3 shows the XRD patterns of $Cd_{0.6}Zn_{0.4}S$ and Ru doped $Cd_{0.6}Zn_{0.4}S$ prepared by co-precipitation method. All the samples exhibit major diffraction peak at 2θ of 27.25º, 45º, 52º ($Cd_{0.6}Zn_{0.4}S$) and 28.05º, 42.53º, 51.36º ($Ru/Cd_{0.6}Zn_{0.4}S$), corresponding to the (111), (220) and (311) planes of cubic zinc blende phase. However, it is clear that the XRD peaks were broadened as the 1 % of Ru dopant in the entire sample that would be due to the presence of hexagonal phase. It is well known that $Cd_{0.6}Zn_{0.4}S$ can exit in both hexagonal and cubic phases. It was revealed that hexagonal phase was observed when the amount of Zn in $Cd_{0.6}Zn_{0.4}S$ was small. In the present study, we also obtained that the hexagonal phase was formed when the amount of Zn

decreased due to the increased of Ru dopant amount. Based on the calculation by Scherrer equation, crystalline size decreased as the amount of Ru dopant in the $Cd_{0.6}Zn_{0.4}S$. The doped catalyst $Ru/Cd_{0.6}Zn_{0.4}S$ had higher (2θ) values than the non-doped catalyst. Particularly, the 2θ value of the peak clearly showed that ruthenium doping in the entire composite of the photocatalyst. The peak clearly showed that the doped catalyst was slightly merged with the non-doped catalyst. It clearly indicated the complete coverage of Ru doping by outer layer of $Cd_{0.6}Zn_{0.4}S$ mantle.
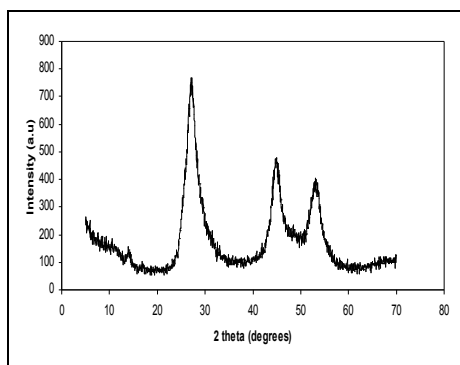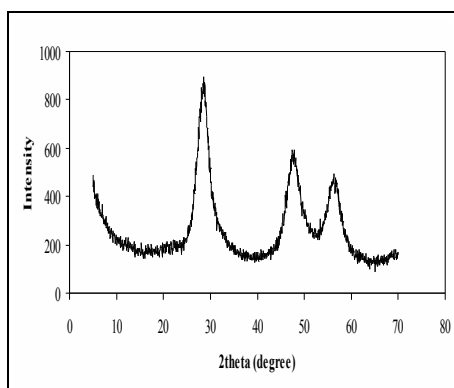

Fig. 2 XRD pattern of $Ru/Cd_{0.6}Zn_{0.4}S$

Fig. 3 XRD pattern of $Cd_{0.6}Zn_{0.4}S$

B. SEM characterization (morphology)

Scanning electron microscope (SEM) used to determine the morphology of $Ru/Cd_{0.6}Zn_{0.4}S$ as shown in Fig. 4. It can be observed that the sample consisted of nanosphere in the range of 10- 200 nm, which agglomerated with no uniform size. It was noticeable that the catalyst showed aggregates of tiny plates like crystalline and irregular shaped particles. All of them were dense aggregate. The Ru co-catalyst deposits was seen in the image as white spots/patches. The particle size was observed of 10-200 nm on the catalyst surface. Gurunathan et al.,2008 and Preethi and Kanmani, 2012also have noticed in the SEM image the white spots of $RuCl_2$ catalyst particles of 10-50 nm and 200 – 300 nm size on the catalyst surface.
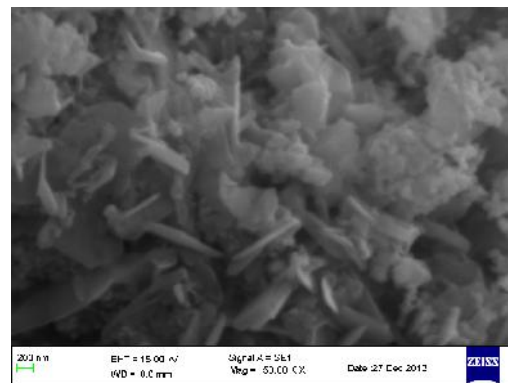

Fig. 4. SEM image of $Ru/Cd_{0.6}Zn_{0.4}S$

C. UV-DRS characterization (band gap)

DRS UV-Vis spectra of $Ru/Cd_{0.6}Zn_{0.4}S$ and $Cd_{0.6}Zn_{0.4}S$ photocatalyst were shown in Fig. 5. ZnS has an absorption band in the ultraviolent region, and CdS reaches the visible light region with an absorption band at about 500 nm. The addition of Ru dopant extended the visible light absorption of $Cd_{0.6}Zn_{0.4}S$ to longer wavelength. The absorption edge of $Cd_{0.6}Zn_{0.4}S$ was about 475 nm, whereas $Ru/Cd_{0.6}Zn_{0.4}S$ was about 450 nm. After doping, threshold and band gap energy changed due to incorporation of Ru doped to the $Cd_{0.6}Zn_{0.4}S$. From the several literature reviews, the coherent absorption in the wavelength range of 200-650 nm suggests that the optical electronic transition involves only VB and CB. The reflectance edge for the two catalysts increases with one point at 450 and 475 nm that correspond to the band gap energies of 2.8 and 2.63 eV, respectively. The band gap was calculated by using formula $E_{bg}=1240/λ$ in eV (Bhatkande et al., 2001 and Reddy *et al.*, 2002).
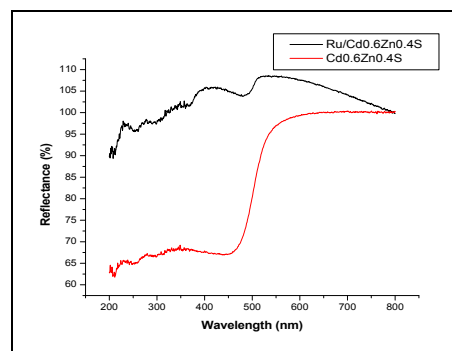

Fig. 5. UV-DRS for $Ru/Cd_{0.6}Zn_{0.4}S$

D. Composition by EDX

EDS pattern of naked catalyst $RuCl_2$ loaded $Cd_{0.6}Zn_{0.4}S$ was shown in Fig. 6. The added composition (during the preparation of photocatalyst) was matching with the composition of elements analyzed in the nanophotocatalyst. This means there was no loss after the calcination of the sample. The EDS spectrum images show the presence of Cd, Zn, Ru and S in the $Ru/Cd_{0.6}Zn_{0.4}S$ nanophotocatalyst.
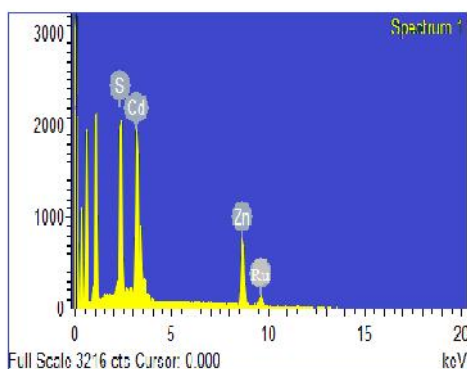
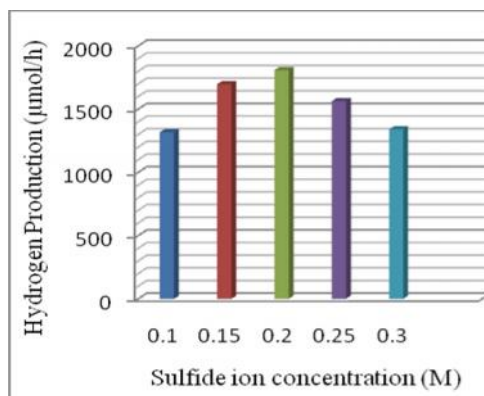Fig. 6. EDS spectrum image for Ru/Cd$_{0.6}$Zn$_{0.4}$S

Fig.7. Effect of sulfide ion concentration

Fig. 8. Effect of sulfite ion concentration

E. Photocatalytic evolution of hydrogen

The photocatalytic hydrogen production from Ru doped Cd$_{0.6}$Zn$_{0.4}$S nanophotocatalyst was conducted in aqueous solutions under visible light irradiation. To achieve optimised photocatalytic activity, the concentration of the sacrificial reagents was varied. Fig. 7 & 8 displays the hydrogen generation rate on the concentration of the sacrificial agents. The mechanism of using Na$_2$S and Na$_2$SO$_3$ as the sacrificial reagents in the aqueous solution to produce H$_2$ from simulated sulfide wastewater can be expressed in the equation (1) – (5). The occurrence of reaction (2) – (5) was verified by the detection of S$_2^{2-}$ and S$_2$O$_3^{2-}$ species in the reaction mixture after photoreaction. When the concentration of Na$_2$SO$_3$ was fixed at 0.25 M, the experiments were conducted at optimizing the sulfide concentration because the sulfide ion concentration found to be the best sacrificial agents as they can act as hole scavengers. The concentration of sulfide ion has a significant influence on the generation of H$_2$ was studied at different sulfide ion concentration in the range of 0.1- 0.3 M. Among that, the higher hydrogen generation was attained at the concentration of 0.2 M. Further increases from concentration of 0.25 M - 0.3 M, there is a decrease in hydrogen production. The result of the study is depicted in Fig. f. This is due to the increase in concentration of polysulfide ion which absorbs part of the visible light. Both sulfide and sulfite ions behaved as quenching agents of ions and radicals [Cui et al., 2004].

At the beginning of the reaction, the rate of hydrogen production was higher in the presence of S^{2-} ions than in a solution containing SO$_3^{2-}$ ions (1). The rate of hydrogen in the solution containing S^{2-} ions decreased due to the formation of disulfide ions, which complete with the proton reduction (2). The yellow disulfide acts as optical filter, reducing the light absorption [Priya and Kanmani, 2008 and Raj Kumar Arya. 2012]. The addition of sulfite ion to sulfide ions, suppresses the photocorrosion because the sulfite concentration plays a significant role in erratic behaviour of sulfide nature. The added sulfite ions combine with polysulfide and produce thiosulphate given in equation 3-5. The optimum concentration of sulfite ion was found at 0.25 M. Further increase concentration from 0.25-0.3 M, decreases the generation of hydrogen as shown in Fig. g. It is due to the competitive absorption of sulfide and thioulfate on the active site of the photocatalyst [Priya and Kanmani, 2008, Cui et al., 2004 and Grzyll et al., 1989].
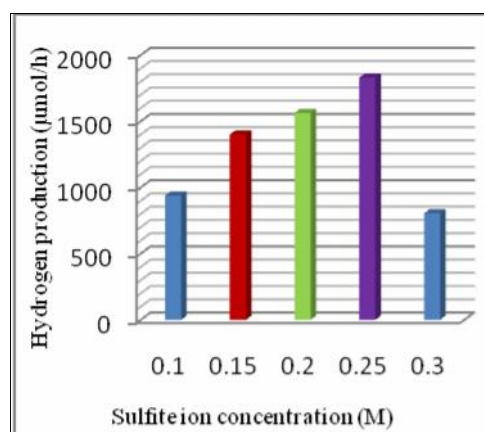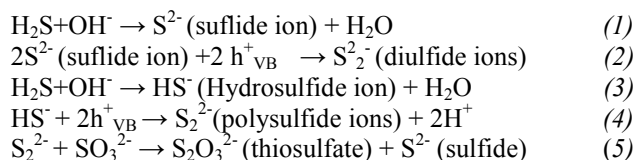
$$H_2S+OH^- \rightarrow S^{2-} \text{ (suflide ion)} + H_2O \qquad (1)$$
$$2S^{2-} \text{ (suflide ion)} +2 \ h^+_{VB} \rightarrow S_2^{2-} \text{ (diulfide ions)} \qquad (2)$$
$$H_2S+OH^- \rightarrow HS^- \text{ (Hydrosulfide ion)} + H_2O \qquad (3)$$
$$HS^- + 2h^+_{VB} \rightarrow S_2^{2-} \text{(polysulfide ions)} + 2H^+ \qquad (4)$$
$$S_2^{2-} + SO_3^{2-} \rightarrow S_2O_3^{2-} \text{ (thiosulfate)} + S^{2-} \text{ (sulfide)} \qquad (5)$$

Volume of hydrogen produced with change in catalyst loading can be seen in Fig. 9. At the low concentration the rate of hydrogen production increases with increase in photocatalyst loading from 0.1 g to 0.2 g as the screening effect are negligible. At higher loading 0.2 to 0.5 g, the screening effects happened significantly and thus the rate drops very rapidly [Priya and Kanmani, 2008, Linkous et al., 2006, Raj Kumar Arya. 2012 and Preethi and Kanmani, 2014]. Following the sulfite, sulfide and catalyst dosage optimization, pH optimization should be perofrmed because of its prominent role in existing nature of the sulfur compounds. From the pH 9-11, maximum hydrogen production was noted in Fig. 10. Between pH 12-13, the hydrogen production decreased. It was due to the increase of OH- ion concentration. When the hydroxide ions concentration becomes too high, many photogenerated hydrogen ions interacted with hydroxide ions producing water [Priya and Kanmani, 2008, Strataki et al., 2010 and Bao et al., 2008].
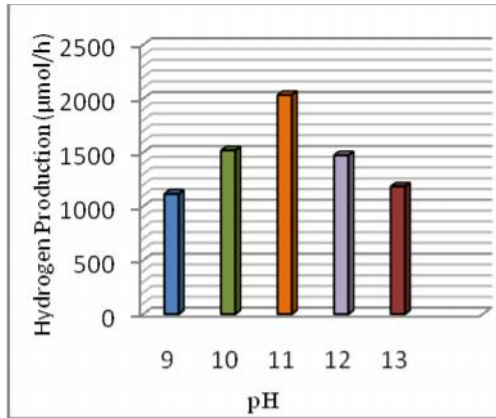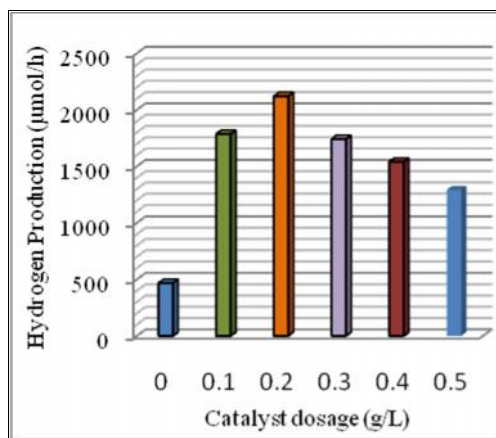
Fig.9. Effect of pH

Fig.11. Effect of volume of sulfide wastewater

Fig.10. Effect of catalyst dosage

Fig.12. Effect of light intensity

The increase in volume of sulfide wastewater from 100-300 mL, the generation of hydrogen decreased was illustrated in Fig. 11. This is due to the reduced less penetration of light into the solution [Priya and Kanmani, 2008 and Huang et al., 2011]. In order to study the light intensity on hydrogen production, the experiments were conducted by varying lamp source at 100 to 300 W. From the Fig. 12, it was observed that, as the intensity of the light increases hydrogen production also increased. This is due to the formation of large number of electron/hole pairs [Linkous et al., 2006, Preethi and Kanmani., 2014 and Rita et al., 2010].

The photocatalytic experiments were repeated five times with the same catalyst. After each experiment, the nanophotocatalyst was filtered, washed, dried and use it again for experiments. For each consequent trial the volume of H_2 generated, decreased gradually. The decrease of photocatalyst activity might be due to the loss of the catalyst during washing and filtration process combined with a small quantity of photocorrosion in the catalysts [Priya and Kanmani, 2008, Preethi and Kanmani, 2014 and Rita et al., 2010].This suggests that fresh catalyst loading might be required to compensate the loss after few runs in Fig. 13.
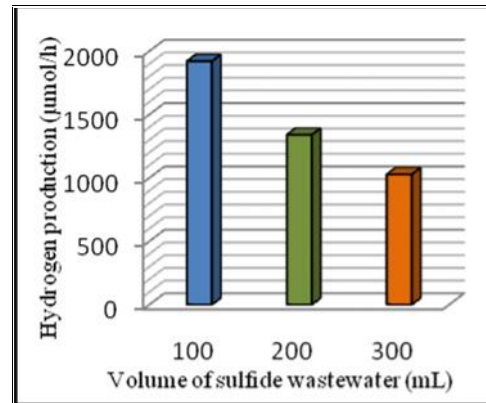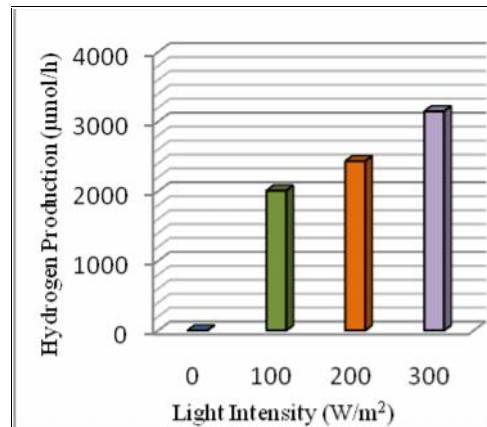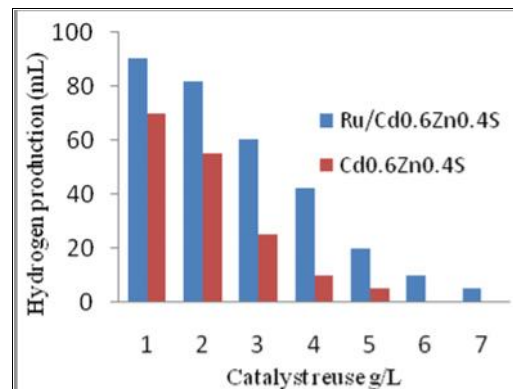

Fig.13. Effect of catalyst reuse

The feasibility studies were carried out with the optimizing all the operating parameters, the performance of the reactors were compared with the existing catalysts. By carrying out the experiment for the optimized condition of 0.2 M of sulfide ion concentration, 0.25 M of sulphite ion concentration, 0.2 g of catalyst dosage, pH of 11, lamp source of 300 W and volume of sample 100 mL, the H_2 generation rate was 90.5 mL for trapezoidal reactor and 71 mL for cylindrical tapered bottom reactor, the results are shown in Fig. 14. The trapezoidal reactor had flat surface to absorb the direct solar radiation this leads to higher rate of H_2 production. The cylindrical reactor had flat bottom and the catalyst was settled at the bottom of the nozzle and the sunlight could not directly penetrate into the reactor, this lead to the lower rate of H_2 production.
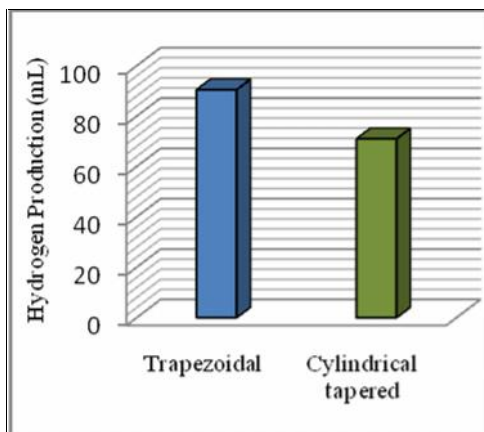
Fig.14. comparison on two reactors

IV. CONCLUSION

In summary, Ru doped Cd$_{0.6}$Zn$_{0.4}$S photocatalysts were prepared by co-precipitation method and also studied photocatalytic hydrogen production under visible light irradiation. The characterization of the catalyst clearly reveals that the photocatalyst is present in the most active form. The catalyst was also subjected to reuse and evaluated for its efficiency in each trial wherein the catalyst has shown photostability upto five trials. The preparation method of catalyst is easy and reproducible. From the results, it is concluded that trapezoidal reactor was better than cylindrical tapered bottom reactor.

Results obtained from this research indicate that the synthesized photocatalyst Ru/Cd$_{0.6}$Zn$_{0.4}$S in trapezoidal reactor, when coupled with batch process with continuous mixing has effectively decomposed H$_2$S in alkaline solution with the generation of H$_2$ gas, which could be used as clean fuel. Hydrogen is a product that is fully capable of sustaining the world's energy needs now and in the future. If renewably produced, H$_2$ would be a fuel used that does not contribute to environmental damage (pollution) and supports the human well being.

REFERENCES

[1] Priya, R. and Kanmani, S. (2008). Solar photocatalytic generation of hydrogen from hydrogen sulphide using CdS-based photocatalysts. Current Science, 94, 102-104.

[2] Gurunathan, K., Baeg, J., Lee, S., Subramanian, E., Moon, S. and Kong, K. (2008). Visible light assisted highly efficient hydrogen production from H$_2$S decomposition by CuGaO$_2$ and CuGa$_{1-x}$In$_x$O$_2$delafossite oxides bearing nanostructured co-catalysts. Catalyst Community, 9, 395-402.

[3] Niranjan Biswal., Das, D. P., Satyabadi Martha. and Parida, K.M. (2011). Efficient Hydrogen Production by Composite Photocatalyst CdS/ ZnS, Zirconium – Titanium Phosphate (ZTP) under visible light illumination. International journal of hydrogen energy, 36, 13452-13460.

[4] Preethi, V. and kanmani, S. (2012). Photocatalytic hydrogen production over CuGa$_2$ – Fe$_x$O$_4$/RuO$_2$ spinel. International journal of hydrogen energy, 37, 18740-18746.

[5] Linkous, C.A., Huang, C. and Fowler, R. (2006). UV photochemical oxidation of aqueous sodium sulfide to produce hydrogen and sulphur. Journal of Photochemical Photobiology A: Chemistry, 168, 153-160.

[6] Nada, A.A., Hamed, H.A., Barakat, M.H. and Mohamed, N.R. (2008). Enhancement of photocatalytic hydrogen production rate using photosensitized TiO^2/RuO^2-MV^{+2}. International journal of hydrogen energy, 33, 3264-3269.

[7] Priya, R. and Kanmani, S. (2010). Solar photocatalytic generation of hydrogen under ultraviolet-visible light irradiation on (CdS/ZnS)/Ag$_2$S + (RuO$_2$/TiO$_2$) photocatalysts. Building Material Science, 33, 85-88.

[8] Xianghui Zhang., Dengwei Jing. and Liejin Guo. (2010). Effects of anions on the photocatalytic H$_2$ production performance of hydrothermally synthesized Ni-doped Cd$_{0.1}$Zn$_{0.9}$S photocatalysts. International journal of hydrogen energy, 35, 7051-7057.

[9] Xiaojing Liu., Peng Zeng., Tianyou Peng., Xiaohu Zhang. and Kejian Deng. (2011). Preparation of multiwalled carbon nanotubes/ Cd$_{0.8}$Z$_{02}$S nano composite and its photocatalytic hydrogen production under visible light. International journal of hydrogen energy, 34, 1375-1384.

[10] Supriya, V., Tambwekar, D. and Subrahmanyam, M. (1997). Photocatalytic generation of hydrogen from hydrogen sulfide an energy bargain. International. Journal of hydrogen energy, 22, 959-965.

[11] Naixu Li., Bingyao Zhou., Penghui Guo. and Jiancheng Zhou. (2013). Fabrication of noble metal free Cd$_{0.5}$Zn$_{0.5}$S/NiS hybrid photocatalyst for efficient solar hydrogen evolution. International journal of hydrogen energy, 38, 11268-11277.

[12] Bhatkande, D.S., Pangarkar, V.G. and Beenackers, A.A. (2001). Photocatalytic degradation for environmental applications – a review. Journal of Chemistry, Technology and Biotechnology, 77, 102-116.

[13] Reddy, K.M., Panorama, S.V. and Reddy, A.R. (2002). Bandgap Studies on anatase titanium dioxide nanoparticles. Material Chemistry Physics, 78, 239-245.

[14] Cui, W., Feng, L., Xu, C., Lu, S. and Qiu, F. (2004). Hydrogen production by photocatalytic decomposition of methanol gas on Pt/TiO$_2$ nano-film. Catalyst Community, 5, 533-536.

[15] Raj Kumar Arya. (2012). photoelectrochemical hydrogen production using visible light. International Journal of Hydrogen Energy, 02.

[16] Grzyll, L.R., Thomas, J.J. and Barile, R.G. (1989). Photo electrochemical conversion of hydrogen sulfide to hydrogen using artificial light and solar radiation. International journal of Hydrogen Energy, 14, 647-651.

[17] Preethi, V. and kanmani, S. (2014). Photocatalytic hydrogen production using Fe$_2$O$_3$ based nanoprticle with ZdS and CdS. International Journal of Hydrogen Energy, 39, 1612-1622.

[18] Strataki, N, Antoniadou, M, Dracopoulos, V. and Lianos, P. (2010). Visible light photocatalytic hydrogen production from ethanol water mixtures using a Pt-CdS-TiO$_2$ photocatalys. Catalyst Today, 151, 53-57.

[19] Bao, N.Z., Shen, L.M., Takata, T. and Domen, K. (2008). Self-templated synthesis of anoporous CdS nanostructures for highly efficient photocatalytic hydrogen production under visible light. Chemistry Material, 20, 110-117.

[20] Huang, C., Yao, W., T-Raissi, A. and Muradov, N. (2011). Development of efficient photoreactors for solar hydrogen production. Solar Energy, 85, 19-27.

[21] Rita, J. and Sasi Florence, S. (2010). Optical, structural and morphological studies of bean-like ZnS nanostructures by aqueous chemical method. Chalcogenide Letters, 7, 269-273.

[22] Jing, D., Guo, L., Zhao, L., Zhang, X., Liu, H., Li, M., Shen, S., Liu, G., Hu, X. and Guo, P. (2010). Efficient solar hydrogen production by photocatalytic water splitting: From fundamental study to pilot demonstration. International Journal of Hydrogen Energy, 35, 7087-7097.

[23] Lu Wang., Wenzhong Wang., Meng Shang., Wenzong Yin., Songmei Sun. and Ling Zhang. (2010). 'Enhanced photocatalytic hydrogen evolution under visible light over Cd$_{1-x}$Zn$_x$S solid solution with cubic zinc blend phase', International Journal Hydrogen Energy, Vol. 35, pp. 19 -25.

[24] Yabo Wang., Jinachumwu., Jianwei Zheng., Rongrong Jiang. and RongXu. (2012), 'Photocatalysts from single source precursors for efficient solar hydrogen production under visible light irradiation', Catalysis Science and Technology, Vol. 2, pp.581-588.

[25] Guanji Liu. (2008) 'Photocatalytic H$_2$ evaluation under visible light irradiation on a novel Cd$_X$Cu$_y$Zn$_{1-X-Y}$ S catalyst'.

N.Thangam working as assistant professor in SRR Engineering College completed my bachelor degree in Civil Engineering in Periyar Maniammai University and master degree in Environmental Management in Anna University, Chennai.

B.Suganya Devi working as assistant professor in SRR Engineering College completed my bachelor degree in Civil Engineering in PSNA and master degree in Environmental Engineering in Anna University, Chennai.

A.C. Lalitha Muthu working as assistant professor in SRR Engineering College completed my bachelor degree in Civil Engineering in Raja College of engineering and technology and master degree in Irrigation water management in Anna University, Chennai. Research work in "Land use and Land cover changes".